

Influence of isoelectronic substitutions on the magnetism of UCoAl

Alexander V. Andreev*

Institute of Physics ASCR, Na Slovance 2, 18221 Prague, Czech Republic

Nikolai V. Mushnikov

Institute of Metal Physics, Kovalevskaya 18, 620219 Ekaterinburg, Russia

Martin Diviš, Fuminori Honda,[†] and Vladimír Sechovský

Faculty of Mathematics and Physics, Department of Electronic Structures, Charles University, Ke Karlovu 5, 12116 Prague, Czech Republic

Tsuneaki Goto

Institute for Solid State Physics, University of Tokyo, Kashiwanoha 5-1-5, Kashiwa, Chiba 277-8581, Japan

(Received 18 October 2004; published 31 March 2005)

UCoAl has a paramagnetic ground state but exhibits a susceptibility maximum and a metamagnetic transition at low magnetic fields applied along the hexagonal c axis. This behavior is easily changed by small substitutions in the nonmagnetic Co sublattice with suitable elements to ferromagnetism (Mn, Fe, Ru, Rh, or Ir) or to conventional paramagnetism (Ni, Cu, Pd, or Pt). Here the influence on magnetism from the simultaneous substitution of Co by equal amounts of Ni and Fe, $\text{UCo}_{1-z}(\text{Ni}_{0.5}\text{Fe}_{0.5})_z\text{Al}$ has been studied by magnetization measurements at ambient and high pressures on single crystals with $z=0.1$ and 1. This substitution was chosen so that it maintained the average number of d electrons constant. However, despite the constant number of $3d$ electrons with increasing z , stabilization of ferromagnetism is observed. This is attributed to the anisotropic change in lattice parameters upon substitution, which is consistent with results of the magnetostriction and uniaxial-pressure magnetization measurements of UCoAl. The ferromagnetic ground state of $\text{UNi}_{0.50}\text{Fe}_{0.50}\text{Al}$ ($z=1$) is corroborated by first-principles electronic-structure calculations in the framework of the density functional theory.

DOI: 10.1103/PhysRevB.71.094437

PACS number(s): 75.30.Kz, 46.25.Hf

I. INTRODUCTION

The uranium intermetallic compound UCoAl (hexagonal structure of the ZrNiAl type) has a paramagnetic ground state but exhibits a susceptibility maximum and a metamagnetic transition (MT) in magnetic field applied along the hexagonal c axis.¹⁻³ In many of its properties, the magnetic behavior of UCoAl resembles that of YCo_2 and its related compounds in a small group of $3d$ -band metamagnets.⁴ In YCo_2 , the $3d$ electrons of Co are responsible for the magnetism, whereas UCoAl is a $5f$ -band metamagnet. The magnetization jump $\Delta M=0.3\mu_B$ at the MT is attributed almost completely to U, whereas the Co atoms do not carry a noticeable magnetic moment. The MT in UCoAl is observed at a critical field B_c as low as 0.67 T (compare with 70 T in YCo_2). The specific behavior of UCoAl is easily changed to ferromagnetism or conventional paramagnetism by doping with suitable elements.⁵⁻⁷ The B_c value is shifted to 2.5 T by a 5% Ni substitution for Co (accompanied by reduction of the magnetization jump), and the MT disappears with further increasing Ni content. A qualitatively similar effect was observed upon Cu, Pd, or Pt substitution, i.e., in the cases when the total number of d electrons increases, which leads to a weakening of the $5f$ - d hybridization. On the other hand, only 2% Fe doping yields a reduction of B_c to zero and the stabilization of a ferromagnetic ground state. Similar effects were observed for other substitutions with decreasing numbers of d electrons (Mn or Ru) or upon the isoelectronic substitu-

tions when the $3d$ metal Co is replaced by $4d$ (Rh) or $5d$ (Ir) metals. In these cases the $5f$ - d hybridization is believed to increase.

It was shown that the number of d electrons plays a more important role in the modification of metamagnetism in UCoAl than varying the interatomic distances because the drastic changes occurs at low doping content while the lattice parameters remain unchanged within the experimental error of x-ray analysis. Nevertheless, application of rather low hydrostatic pressure suppresses the substitution-induced ferromagnetism and causes a reentrance of MT.⁸ The interplay between doping and pressure effects was studied in details on $\text{UCo}_{1-x}\text{T}_x\text{Al}$ ($T=\text{Fe}, \text{Ni}$) single crystals.^{9,10}

In the present work, we substituted Co in UCoAl simultaneously by equal amounts of Ni and Fe and therefore did not change the $3d$ electron concentration. In this case, the variation of the interatomic distances is expected to become the most important factor in determining the magnetic state of the compound. We studied the magnetization at ambient and high pressures on $\text{UCo}_{1-z}(\text{Ni}_{0.5}\text{Fe}_{0.5})_z\text{Al}$ single crystals with $z=0, 0.1$, and 1. It is worth noting that the substitutions are carried out within the nonmagnetic Co sublattice. The experimental results are compared with the results of relativistic electronic structure calculations based on the density functional theory. The disorder within the nonmagnetic Co sublattice is described by the virtual crystal approximation.

TABLE I. Structural and the ambient-pressure magnetic characteristics of the compounds studied.

Compound	a (pm)	c (pm)	M_s (μ_B)	T_C (K)	T_{\max} (K)	B_c (T)
UCoAl	668.6	396.6			20	0.65
UCo _{0.90} Ni _{0.05} Fe _{0.05} Al	669.9	396.5	0.17	16		
UNi _{0.50} Fe _{0.50} Al	674.1	394.7	0.62	52		

II. EXPERIMENTAL DETAILS

Single crystals of UCoAl, UCo_{0.90}Ni_{0.05}Fe_{0.05}Al, and UNi_{0.50}Fe_{0.50}Al were grown by a modified Czochralski method from the melt of stoichiometric amounts of the constituent elements (U of 3N5, Al of 5N, and transition metals of at least 3N5 purity) in a tetra-arc furnace. Samples of nearly cubic shapes of dimensions $\sim 1.8 \text{ mm}^3$ and masses $\sim 60 \text{ mg}$ were spark-erosion cut perpendicular to the principal axes.

The magnetization along the c axis was measured using an extraction-type magnetometer equipped with a 7 T superconducting magnet in a temperature interval 1.5–100 K. For measurements under high pressure, the sample was placed in a Teflon capsule filled with a liquid pressure medium that was a mixture of two types of Fluorinert (FC 70:FC 77 = 1:1), and compressed using a nonmagnetic, piston-cylinder pressure cell made of a Ti-Cu alloy. The maximum available pressure was 1.2 GPa (at low temperatures).

The temperature dependence of magnetic susceptibilities along the a and c axes were measured in a PPMS-9 (Quantum Design) cryomagnetic installation between 2 and 300 K.

III. RESULTS AND DISCUSSION

A. Experiment

X-ray powder diffraction and microprobe analysis of the top, center, and bottom parts of the crystals indicated that they are single phase with the ZrNiAl-type structure and have a homogenous distribution of the components over the sample volume. The lattice parameters of the compounds studied are listed in Table I together with their magnetic characteristics.

Figure 1 shows the temperature dependences of the magnetic susceptibility of the UCo_{1-z}(Ni_{0.5}Fe_{0.5})_zAl crystals measured along the principal axes. Similar to UCoAl, the substituted crystals exhibit a huge magnetic anisotropy. This anisotropy is the major difference from the $3d$ -band metamagnets, which are essentially isotropic. Whereas the c -axis susceptibility curves at high temperature are described by modified Curie-Weiss law with effective magnetic moment 1.85, 1.88, and 2.20 μ_B/U for $x=0, 0.1$, and 1, respectively, the basal-plane susceptibility is much smaller and only weakly temperature dependent irrespective of the ground state of the compound (UCoAl is a paramagnet, UNi_{0.5}Fe_{0.5}Al is a ferromagnet and UCo_{0.90}Ni_{0.05}Fe_{0.05}Al has a mixed state with a ferromagnetic component, see below). Magnetization curves along the a axis are linear up to at least

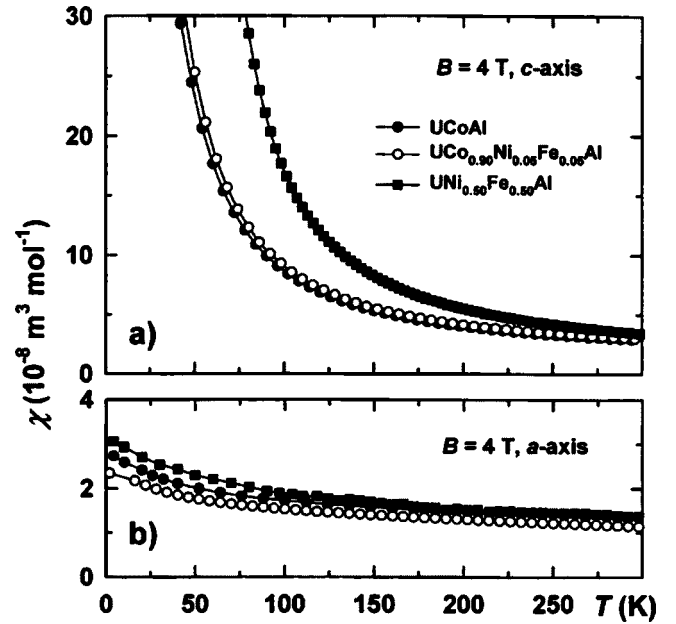


FIG. 1. Temperature dependence of the magnetic susceptibility of the UCo_{1-z}(Ni_{0.5}Fe_{0.5})_zAl crystals in magnetic field of 4 T applied along the c axis (a) and the a axis (b).

40 T for all three compounds. We will only discuss the magnetization with fields applied along the c axis.

The metamagnetic properties of UCoAl are illustrated in Fig. 2. At ambient pressure, the magnetization curve exhibits a magnetization jump $\Delta M=0.3\mu_B$ at $B_c=0.67 \text{ T}$. This has a hysteresis $\Delta B_c=0.05 \text{ T}$ showing that the transition is of first order [Fig. 2(a)]. Under external hydrostatic pressure, the transition remains qualitatively the same, but shifts to higher fields with a rate $dB_c/dP=2.6 \text{ T/GPa}$ and becomes broader. The temperature dependence of the magnetic susceptibility in a field below the metamagnetic transition [Fig. 2(b)] shows a characteristic broad maximum around 20 K. Its height decreases under pressure, and the position moves to higher temperatures.

Figure 3 shows the virgin magnetization curves and demagnetizations of the hysteresis loops of the UCo_{0.90}Ni_{0.05}Fe_{0.05}Al crystal measured along the c axis at different temperatures. The specific shape of the curves can be considered as a superposition of spontaneous ferromagnetic and metamagnetic components of approximately equal magnitudes. The ferromagnetic component is characterized by a pronounced hysteresis. The hysteresis properties are typical for ferromagnetic uranium intermetallics with ZrNiAl-type crystal structure [UCoSn,¹¹ UPtAl,¹² UIrAl¹³] and correspond to the model of high intrinsic coercivity of narrow domain wall. In particular, the temperature dependence of the coercive field B_{coer} , shown in the inset of Fig. 3, obeys very well the exponential law

$$B_{\text{coer}}(T) = B_{\text{coer}}(0)\exp(-k_B T/E_{\text{act}}) \quad (1)$$

with parameters $B_{\text{coer}}(0)=0.24 \text{ T}$ and $E_{\text{act}}=4.8 \times 10^{-23} \text{ J}$ (the dashed curve). The activation energy E_{act} is found to be practically the same as in UPtAl ($5.3 \times 10^{-23} \text{ J}$), whereas the

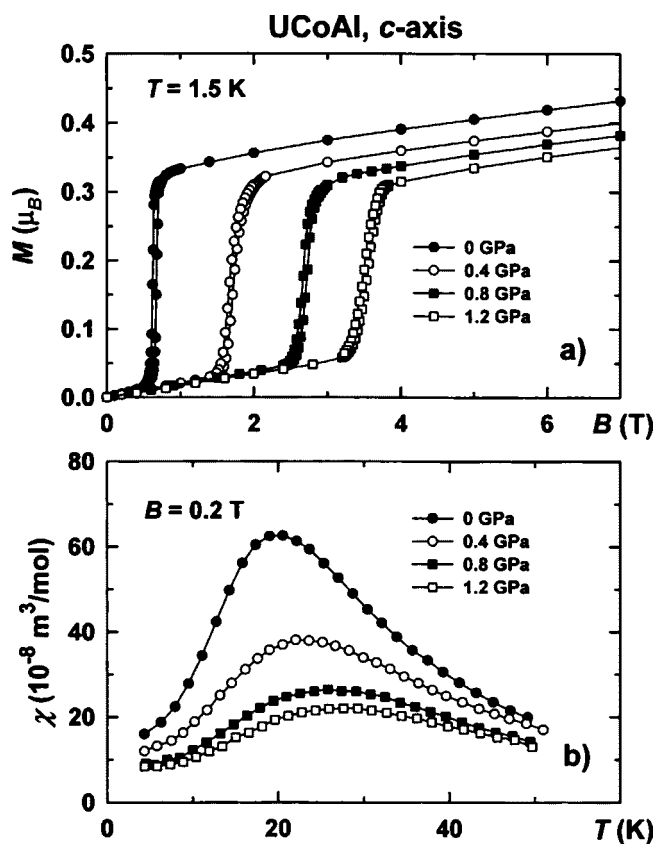


FIG. 2. Magnetic properties of a UCoAl single crystal measured in field applied along the c axis at ambient and elevated hydrostatic pressure. (a). Magnetization curves at 1.5 K. (b) Temperature dependences of magnetic susceptibility in a 0.2 T field.

$B_{\text{coer}}(0)$ value in UPtAl is considerably larger (1.05 T).¹² The latter can indicate a larger anisotropy energy in UPtAl compared to that of $\text{UCo}_{0.90}\text{Ni}_{0.05}\text{Fe}_{0.05}\text{Al}$.

At ambient pressure, the ferromagnetism of $\text{UCo}_{0.90}\text{Ni}_{0.05}\text{Fe}_{0.05}\text{Al}$ vanishes at the Curie temperature $T_C = 16$ K. This ferromagnetic state is rather unstable and can be suppressed by the application of external pressure and the restoration of metamagnetism is observed [Fig. 4(a)]. A pressure as low as 0.4 GPa is enough to shift the critical field B_c from practically zero to 0.7 T as in UCoAl. The only difference between UCoAl at ambient pressure and $\text{UCo}_{0.90}\text{Ni}_{0.05}\text{Fe}_{0.05}\text{Al}$ at 0.4 GPa is that the metamagnetic transition is noticeably broader in the latter case because of some atomic disorder. A similar situation was observed in the off-stoichiometric UCoAl-based crystals $\text{U}_{0.8}\text{Co}_{1.1}\text{Al}_{1.1}$ and $\text{UCo}_{1.1}\text{Al}_{0.9}$.¹⁴ With further increasing pressure, B_c increases at the same rate as in UCoAl, 2.6 T/GPa. Reentrance of the metamagnetism in $\text{UCo}_{0.90}\text{Ni}_{0.05}\text{Fe}_{0.05}\text{Al}$ under pressure is seen also in the evolution of the temperature dependence of the magnetic susceptibility [Fig. 4(b)]. After the characteristic metamagnetic behavior with its broad maximum is restored at 0.6 GPa, the temperature of susceptibility maximum T_{max} increases with increasing pressure at the same rate as in UCoAl, 6 K/GPa.

As shown in Fig. 5 $\text{UNi}_{0.50}\text{Fe}_{0.50}\text{Al}$ is a ferromagnet without any trace of metamagnetism. The virgin magnetization curve and hysteresis loop measured along the easy-

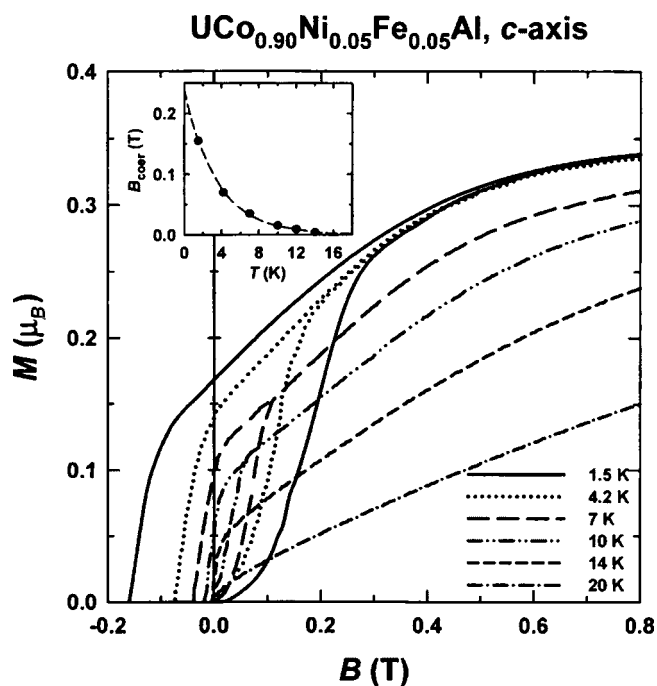


FIG. 3. Virgin magnetization curves and demagnetization part of the hysteresis loops of a $\text{UCo}_{0.90}\text{Ni}_{0.05}\text{Fe}_{0.05}\text{Al}$ single crystal measured along the c axis at different temperatures. The inset shows the temperature dependence of the coercive field B_{coer} (symbols—the experiment points, dashed curve—the exponential fit).

magnetization direction (the c axis) at 1.5 K resembles the behavior of other isostructural ferromagnets^{13–15} or of the ferromagnetic component of $\text{UCo}_{0.90}\text{Ni}_{0.05}\text{Fe}_{0.05}\text{Al}$. The temperature dependence of B_{coer} , shown in the inset of Fig. 5, can be fit by the exponent (1) with parameters $B_{\text{coer}}(0) = 0.34$ T and $E_{\text{act}} = 9.9 \times 10^{-23}$ J. At ambient pressure, $\text{UNi}_{0.50}\text{Fe}_{0.50}\text{Al}$ has spontaneous magnetic moment $M_s = 0.62 \mu_B/U$ and $T_C = 52$ K. These data are in satisfactory agreement with results of Ref. 15 where ferromagnetism in solid solutions between the Pauli paramagnet UFeAl and the itinerant antiferromagnet UNiAl has been reported for the first time on polycrystalline samples.

The ferromagnetism in $\text{UNi}_{0.50}\text{Fe}_{0.50}\text{Al}$ is relatively stable under hydrostatic pressure (Fig. 6). The values of M_s and T_C decrease considerably under pressure ($d \ln M_s / dp = 0.09 \text{ GPa}^{-1}$, $d \ln T_C / dp = 0.14 \text{ GPa}^{-1}$), but no qualitative change occurs up to 1.2 GPa unlike the unstable ferromagnets $\text{UCo}_{0.90}\text{Ni}_{0.05}\text{Fe}_{0.05}\text{Al}$ (Fig. 4) and $\text{UCo}_{0.98}\text{Fe}_{0.02}\text{Al}$.⁸

The number of $3d$ electrons remains unchanged with increasing z , and therefore the strength of the $5f$ - $3d$ hybridization, the main delocalization mechanism of $5f$ electrons, can be also expected to be unchanged. Nevertheless, the effects of the Ni and Fe doping are not symmetric. The Fe doping influences the state of $5f$ electrons stronger, and stabilization of ferromagnetism is observed with increasing z in $\text{UCo}_{1-z}(\text{Ni}_{0.5}\text{Fe}_{0.5})_z\text{Al}$. In order to understand the origin of this asymmetry, one needs to consider the changes in lattice parameters upon substitution. These changes are rather small and their influence is negligible compared to the effect of the variation of the number of $3d$ electrons. However, when this number is constant, the change in the lattice parameters upon

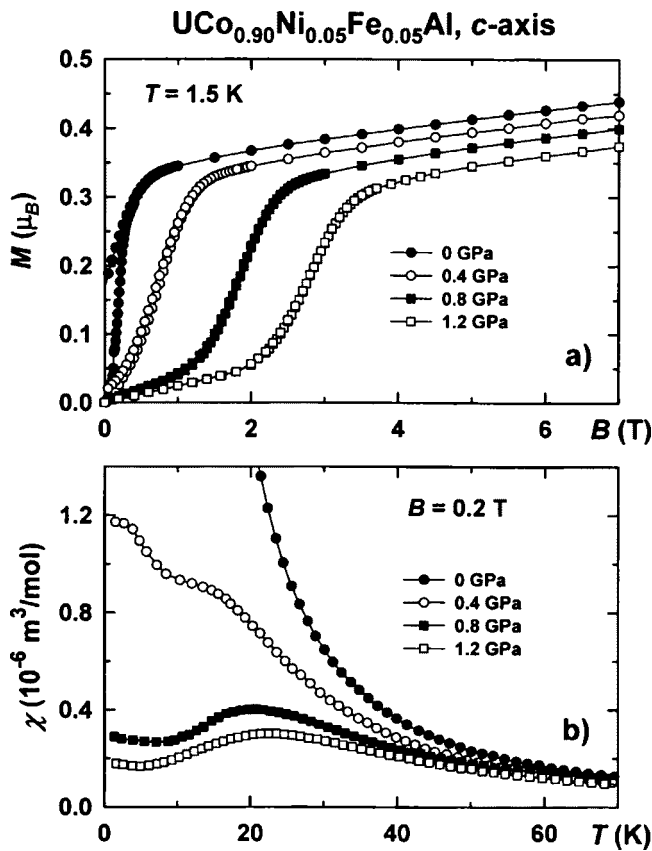


FIG. 4. Magnetic properties of a $\text{UCo}_{0.90}\text{Ni}_{0.05}\text{Fe}_{0.05}\text{Al}$ single crystal measured in field applied along the c axis at ambient and elevated hydrostatic pressure. (a) Magnetization curves at 1.5 K. (b) Temperature dependences of magnetic susceptibility in a 0.2 T field.

substitution became important. Figure 7 shows that the unit cell expands in the basal plane and shrinks along the c axis with increasing z . Similar anisotropic behavior of lattice parameters is observed by the magnetostriction measurements in unsubstituted UCoAl at the metamagnetic transition (the inset in Fig. 7).^{16,17} This also correlates with results of uniaxial-pressure experiments. The ferromagnetism in UCoAl is induced by uniaxial pressure applied along the c axis.^{18,19} Its application along the a axis leads to the opposite effect—increasing B_c .²⁰ The arrow in Fig. 7 corresponds to the critical value z_0 at which the lattice-parameter change reaches the corresponding magnetostriction at the metamagnetic transition in UCoAl . The value of z_0 is estimated to be very low, 0.023 and 0.026 from a and c axes, respectively. This confirms that $\text{UCo}_{0.90}\text{Ni}_{0.05}\text{Fe}_{0.05}\text{Al}$ with $z=0.1$ should already be ferromagnetic.

B. Electronic-structure calculations

For the electronic structure calculations, we used state-of-the-art computational methods, namely, the general-potential augmented plane wave plus local orbitals method (APW+LO, WIEN2K code).²¹ The Kohn-Sham equations were solved within the local-spin-density approximation (LSDA), but in the minimization of the total energy as a function of volume we also tested the influence of the generalized gra-

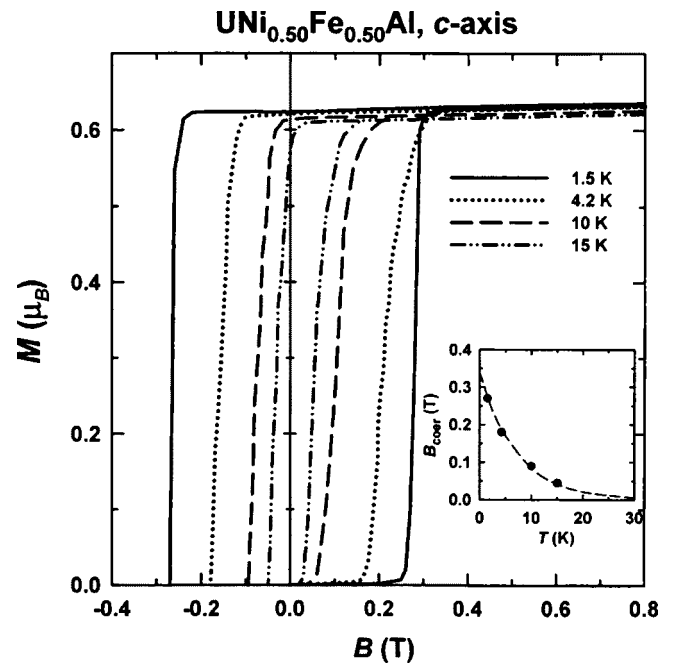


FIG. 5. Virgin magnetization curves and demagnetization part of the hysteresis loops of a $\text{UNi}_{0.50}\text{Fe}_{0.50}\text{Al}$ single crystal measured along the c axis at different temperatures. The inset shows the temperature dependence of the coercive field B_{coer} (symbols—the experiment points, dashed curve—the exponential fit).

dient approximation (GGA).²² The relativistic effects were treated in the scalar relativistic approximation²³ and the spin-orbit coupling (SOC) was self-consistently added via the second variational step scheme.^{23,24} Atomic-sphere (AS) radii of 2.7, 2.3, and 2.1 (2.1) Bohr radii (1 Bohr = 52.9117 pm) were chosen for U, Co, and Al, respectively. We used from 1000 to 1500 augmented-plane-wave basis functions (from about 110 to 160 per atom) in the interstitial region and the maximum $l=12$ in the expansion of the radial wave functions inside the AS to represent the valence states. The uranium $5f$ states were also treated as valence Bloch states, and thus uranium is characterized by a noninteger occupation number. Local orbitals were used to treat the U- $6s$, Co- $3p$, and Al- $2p$ states with the valence states in a single energy window. Relativistic local orbitals for the description of U $6p_{1/2}$ and $6p_{3/2}$ states are included.²⁵ The advantage of this treatment is that the above mentioned semicore states are orthogonal to the valence states. Both the potential and the charge density were expanded inside the spheres into crystal harmonics up to $L=6$ and in the interstitial region into a Fourier series with about 4000 K stars. For the Brillouin zone (BZ) integration, a modified tetrahedron method²¹ with 30–152 special k points in the irreducible wedge (IW) was used to construct the charge density in each self-consistency step. We have carefully checked that with these parameters the calculations converge.

We tested two different implementations of the LSDA+ U method, namely the around mean field (AMF) method and a method with a partial correction to self-interaction.²¹ Since their results are similar, we decided to use the AMF method, because by construction it is better suited for sys-

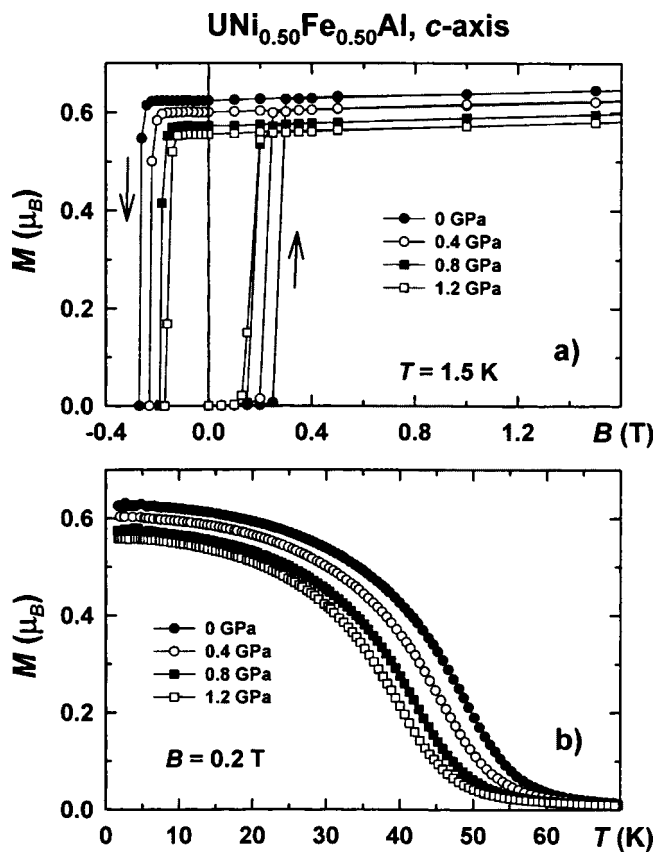


FIG. 6. Magnetic properties of a UNi_{0.5}Fe_{0.5}Al single crystal measured in field applied along the *c* axis at ambient and elevated hydrostatic pressure. (a) Magnetization curves at 1.5 K. (b) Temperature dependences of magnetic moment in a 0.2 T field.

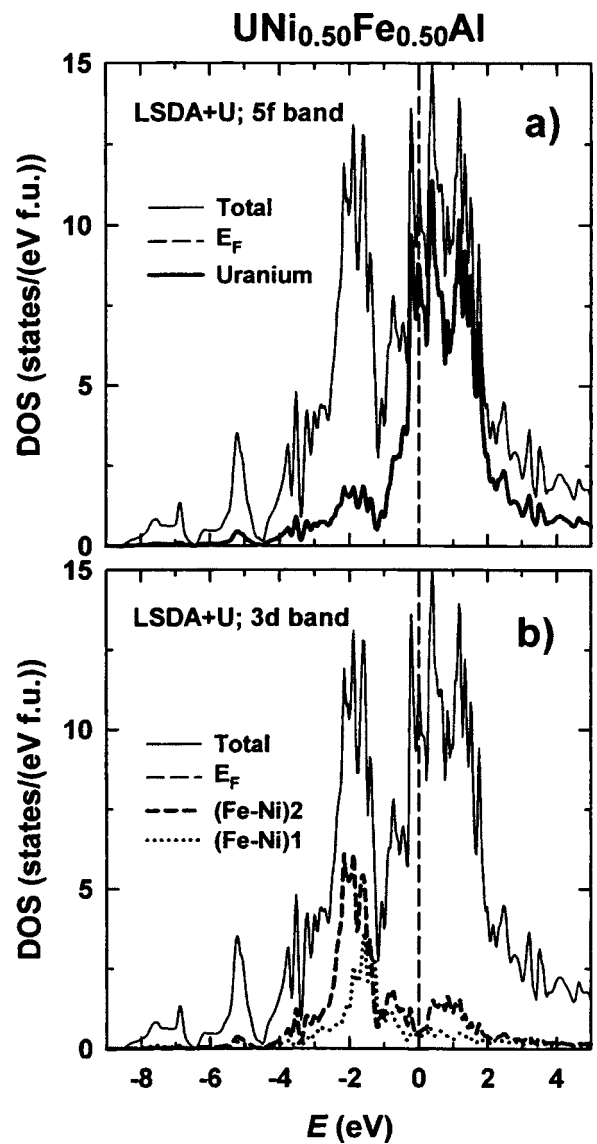


FIG. 8. Electronic structure for UNi_{0.5}Fe_{0.5}Al calculated using LSDA+*U* ($U=0.57$ eV, $J=0.33$ eV) fully relativistic approach (WIEN2K code). The full line shows the total DOS, full thick line [panel (a)] shows the uranium sphere projected DOS, dashed and dotted lines [panel (b)] show the Fe-Ni₂ sphere and the Fe-Ni₁ sphere projected DOS.

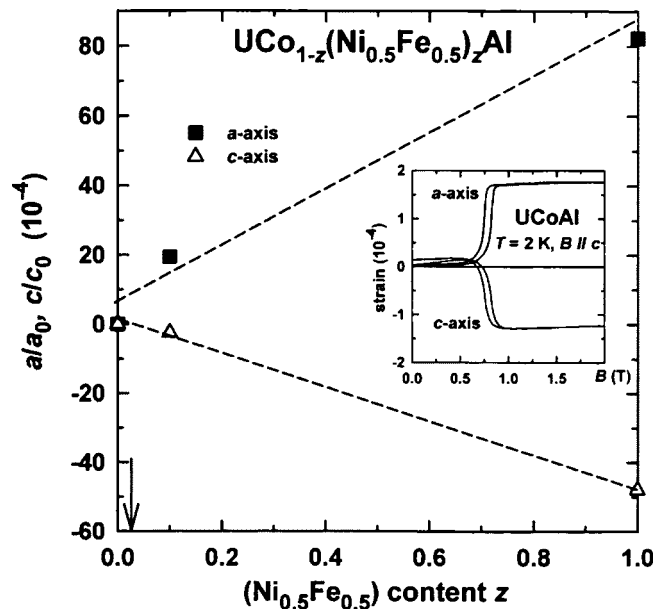


FIG. 7. Concentration dependence of the lattice parameters. In the inset the magnetostriction curves for UCoAl ($z=0$) are shown (Ref. 16).

tems with a lower degree of localization, which should be the case for the UTX compounds. The LSDA+*U* potential is implemented in a rotationally invariant way in both cases. In these calculations, we varied the parameters *U* and *J*, which were used to describe the onsite Coulomb (direct and exchange) interactions inside the 5*f* shell. Considering the atomic values $U=2.0$ eV and $J=0.55$ eV,²⁶ we varied the effective *U* in the range from 0.2 to 1.0 eV with three different *J* values, namely, 0.33, 0.44, and an atomic value 0.55 eV. Optimization of *U* and *J* should lead to the best agreement with the experimental saturated magnetic moment. Assuming that LSDA+*U* is appropriate for description of magnetism of UTX compounds, we *heuristically* expect that the value of *J* does not change dramatically from its atomic value and that the value of *U* should not be lower than the

value of J . We admit, that on this level such a calculation looses its *ab initio* character but on the other hand, we will show that these heuristically derived values allow us to obtain valuable results.

We tested also how much the results of LSDA+ U calculations depend on the starting density matrix, which can be important in calculations of compounds containing rare-earth atoms. Experience has shown that the converged, self-consistent electronic structure does not depend on the starting density matrices in those cases, where the U and J parameters are smaller than the bandwidth of $5f$ states. In the calculated UNi_{0.50}Fe_{0.50}Al compound this bandwidth exceeds 2 eV, which is well above the upper limit of the interval of used U parameters (1 eV).

Contrary to UCoAl, the alloy UNi_{0.50}Fe_{0.50}Al is ferromagnetic in its ground state. We treated this alloy in the virtual crystal approximation (VCA). Experimental structure parameters, which are fairly different from UCoAl, were applied and Fe and Ni elements were replaced by an “average” element, i.e., Co. The ferromagnetic ground state was correctly reproduced by our VCA calculations as well as the value of the experimental magnetic moment $\mu_{\text{exp}}=0.62\mu_B$ using values $U=0.57$ eV and $J=0.33$ eV. The band-structure calculation leading to the correct magnetic moment on uranium sites reveals that the $3d$ bands are narrow (≈ 2 eV, see Fig. 8). Their centers are higher in energy, and their hybridization with $5f$ bands is strong (see Fig. 8).

Finally, we also varied the volume of UNi_{0.50}Fe_{0.50}Al and calculated the total energy to find the theoretical equilibrium. We used the experimental lattice parameters scaled in equidistant steps of 1%. We did not optimize the internal parameters of the structure (x_U, x_{Al}) with respect to the volume variations. Nevertheless, we found the atomic forces calculated at the experimental atomic positions to be quite small, which allowed us to conclude that the atomic positions are not much influenced by the volume variations. The relativistic full-potential APW+LO GGA calculations provided the equilibrium volume $V_{\text{theor}}/V_0=0.98$ (see Fig. 9).

IV. CONCLUSIONS

UCoAl is a $5f$ band metamagnet with a very low transition field (0.6 T) and maximum in the temperature dependence of the magnetic susceptibility at 20 K. This behavior is easily modified, by small substitutions in the nonmagnetic Co sublattice with suitable elements, to ferromagnetism (e.g., by Fe) or to conventional paramagnetism (e.g., by Ni). Influence on the magnetism of simultaneous substitution of Co by equal amounts of Ni and Fe, UCo_{1-z}(Ni_{0.5}Fe_{0.5})_zAl, which

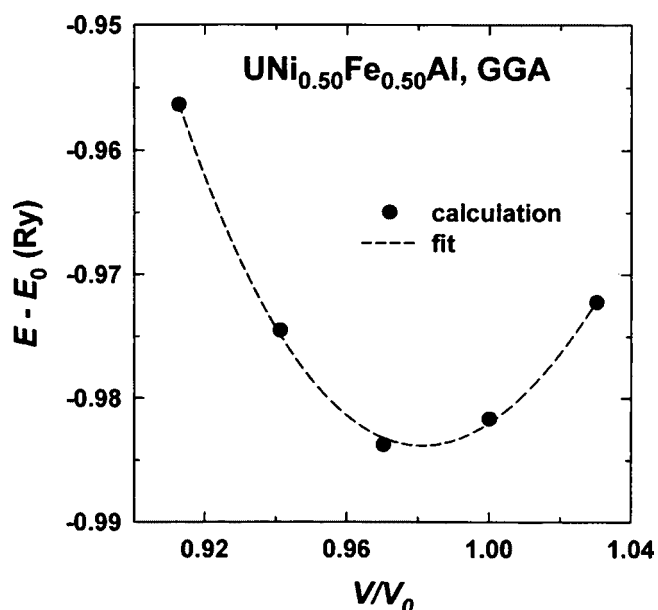


FIG. 9. Total energy calculated as a function of relative volume (V_0 experimental volume) using the generalized gradient approximation (WIEN2K code). The value of $E_0=178315$ Ry.

preserves the isoelectronic state of the system, has been studied in this paper by magnetization measurements at ambient and high pressures on single crystals with $z=0.1$ and 1. In spite of the number of $3d$ electrons remaining unchanged with increasing z , stabilization of the ferromagnetism is observed. This is attributed to an anisotropic change in the lattice parameters upon substitution, which is consistent with results of the magnetostriction and uniaxial-pressure magnetization measurements of UCoAl.

The relativistic full-potential APW+LO LSDA+ U electronic structure calculations reproduced the experimental magnetic moment $\mu_{\text{exp}}=0.62\mu_B$ using values $U=0.57$ eV and $J=0.33$ eV. This points to the importance of the local Coulomb correlations at the uranium site for the description of magnetism of UNi_{0.50}Fe_{0.50}Al compound. The relativistic GGA calculations provided reasonable agreement with the experimental equilibrium volume $V_{\text{theor}}/V_0=0.98$.

ACKNOWLEDGMENTS

This work is a part of the research program MSM 0021620834 that is financed by the Ministry of Education of the Czech Republic. It has been partially supported also by the Grant Agency of the Czech Republic (Grant Nos. 202/02/0739 and 202/03/0550).

*Email address: andreev@mag.mff.cuni.cz

†Present address: Advanced Science Research Center, Japan Atomic Energy Research Institute, Tokai, Ibaraki 319-1195, Japan.

¹V. Sechovský and L. Havela, in *Handbook on Magnetic Materials*, edited by K. H. J. Buschow (Amsterdam, North Holland,

1998), Vol. 11, p. 1, and references therein.

²V. Sechovský, L. Havela, F. R. de Boer, J. J. M. Franse, P. A. Veenhuizen, J. Sebek, J. Stehno, and A. V. Andreev, *Physica B & C* **142**, 283 (1986).

³N. V. Mushnikov, T. Goto, K. Kamishima, H. Yamada, A. V.

- Andreev, Y. Shiokawa, A. Iwao, and V. Sechovský, *Phys. Rev. B* **59**, 6877 (1999).
- ⁴T. Goto, H. Aruga Katori, T. Sakakibara, H. Mitamura, K. Fukamichi, and K. Murata, *J. Appl. Phys.* **76**, 6682 (1994).
- ⁵A. V. Andreev, H. Aruga Katori, and T. Goto, *J. Alloys Compd.* **224**, 117 (1995).
- ⁶A. V. Andreev, L. Havela, V. Sechovský, M. I. Bartashevich, T. Goto, and K. Kamishima, *J. Magn. Magn. Mater.* **169**, 229 (1997).
- ⁷A. V. Andreev, B. Janoušová, M. Diviš, and V. Sechovský, *Physica B* **319**, 199 (2002).
- ⁸N. V. Mushnikov, T. Goto, A. V. Andreev, V. Sechovský, and H. Yamada, *Phys. Rev. B* **66**, 064433 (2002).
- ⁹A. V. Andreev, N. V. Mushnikov, T. Goto, V. Sechovský, Y. Homma, and Y. Shiokawa, *Physica B* **329–333**, 499 (2003).
- ¹⁰N. V. Mushnikov, T. Goto, A. V. Andreev, H. Yamada, and V. Sechovský, *J. Magn. Magn. Mater.* **272–276**, E207 (2004).
- ¹¹A. V. Andreev, *Phys. Met. Metallogr.* **60**, N2, 193 (1985).
- ¹²A. V. Andreev, M. Diviš, P. Javorský, K. Prokeš, V. Sechovský, J. Kuneš, and Y. Shiokawa, *Phys. Rev. B* **64**, 144408 (2001).
- ¹³A. V. Andreev, *J. Alloys Compd.* **336**, 77 (2002).
- ¹⁴N. V. Mushnikov, A. V. Andreev, T. Goto, and V. Sechovský, *Philos. Mag. B* **81**, 569 (2001).
- ¹⁵R. Troc, V. H. Tran, F. G. Vagizov, and H. Drulis, *Phys. Rev. B* **51**, 3003 (1995).
- ¹⁶F. Honda, T. Kagayama, G. Oomi, L. Havela, V. Sechovský, and A. V. Andreev, *Physica B* **284–288**, 1299 (2000).
- ¹⁷A. V. Andreev, R. Z. Levitin, Y. F. Popov, and R. Y. Yumaguzhin, *Sov. Phys. Solid State* **27**, 1145 (1985).
- ¹⁸V. Sechovský, A. V. Andreev, Y. Ishii, M. Kosaka, and Y. Uwatoko, *High Press. Res.* **22**, 155 (2002).
- ¹⁹Y. Ishii, M. Kosaka, Y. Uwatoko, A. V. Andreev, and V. Sechovský, *Physica B* **334**, 160 (2003).
- ²⁰S. R. Saha, H. Sugawara, Y. Aoki, H. Sato, T. D. Matsuda, Y. Haga, E. Yamamoto, and Y. Onuki, *Physica B* **329–333**, 533 (2003).
- ²¹P. Blaha, K. Schwarz, G. K. H. Madsen, D. Kvasnicka, and J. Luitz, WIEN2K, Vienna University of Technology, 2001.
- ²²J. P. Perdew, K. Burke, and M. Ernzerhof, *Phys. Rev. Lett.* **77**, 3865 (1996).
- ²³D. D. Koelling and B. N. Harmon, *J. Phys. C* **10**, 3107 (1977).
- ²⁴J. Kuneš, P. Novák, M. Diviš, and P. M. Oppeneer, *Phys. Rev. B* **63**, 205111 (2001).
- ²⁵J. Kuneš, P. Novák, R. Schmid, P. Blaha, and K. Schwarz, *Phys. Rev. B* **64**, 153102 (2001).
- ²⁶A. B. Shick and W. E. Pickett, *Phys. Rev. Lett.* **86**, 300 (2001).